Modeling of heat transfer to different human cancerous tissues using magnetic nanoparticles

Seyede Nasrin Hsseinimotlagh[1] ,Marzieh Fereshteh[2] , Abuzar Shakeri[3*] ,Mahbubeh Mokhtari[4], Fateme Rasti[5], Mohammad Ali Zarei[6]

[1,2,3,4,5]Department of Physics, Shiraz Branch, Islamic Azad University, Shiraz, Iran

[6]Department of Physics, Payame Noor University, P. O. Box 19395-3697, Tehran, Iran

Abstract

In this paper, we investigate how heat is distributed by three nanoparticles of magnetite, cobalt ferrite and nickel ferrite in five cancer tissue samples by using alternating magnetic field. For this purpose, we first considered a model for heat transfer based on body tissue in a cylindrical coordinate system. Then we drew the related diagrams using Maple software. . Analyzing the results, we found that the temperature transfer in the heat source and near the magnetic nanoparticles is the highest and then decreases. We have also studied the effect of using a continuous Nd-YAG laser at a power of 5 and magnetic nanoparticles and a further increase is observed in the temperature of the damaged tissue. Simultaneous use of lasers and nanoparticles had a remarkable effect on increasing the temperature of cancerous tissue.

Keywords: hyperthermia, tumor, laser, magnetic nanoparticles, tissue, heat

1.Introduction

Abnormal cell proliferation and the body's inability to solve this problem can lead to cancerous tumors. Common treatments for cancer have adverse effects. The use of magnetic nanoparticles under a magnetic field is a promising method in order to treatment of cancer. In this treatment, fluid containing magnetic nanoparticles is injected into the cancerous tissue. After creating an alternating magnetic field, these particles will vibrate. As a result, heat production result in increasing the temperature of the cancerous tissue. The use of magnetic nanoparticles not only improves the performance of chemotherapy but also affects the whole cancerous tissue by heat. So it doesn't leave unheated spot in the cancerous tissue. As we know, with the transition to nanoscale dimensions and changes in surface-to-volume ratio, as well as changes in the distribution of cations and subsequent changes in structural characteristics, nanostructured materials behave differently than volumetric samples This is another reason to use magnetic nanoparticles in heat therapy. [1]

Blood circulation plays an integral role in describing the phenomenon of heat transfer. Without blood circulation, tissue temperature will increase linearly with heating time at a specific heating rate. In the presence of circulating blood flow, the increase in temperature is nonlinear

due to heat loss and the rate of increase in heat decreases until it reaches a steady state. Hence, considering the period of heat loss due to blood circulation, the thermostatic transmission model is established. [2] The parabolic bio heat equation can be traced back to 60 years ago when it was first proposed by the Pennes. Penis modeled heat transfer in a human forearm without movement.[3] Because of metabolism in tissues, heat is generated There is also heat transfer between the blood and adjacent tissues. Therefore, Phrases were added for this purpose. Specific heat, thermal and electrical conductivity, mass density as well as the dielectric constant of the involved biological media tumors, viscera, muscle, fat, skin, etc…should be considered in the model. Another significant element is vascularization. The process of heat transfer highly depends on the blood 's perfusion which is different for tumors and normal tissue. Eventually, heat sources, such as magnetic nanoparticles, must be considered to complete the main tumor model in heat therapy. The body has a large amount of tissue cells. As a consequence, intercellular space should be considered in modeling cancerous tissue.[4] Because cancerous tissues have complex geometries, we need a way to solve the equation to imagine them .In this section, we focus on solving the Pennes equation using cylindrical coordinates. [5] The general form of the Pennes equation is as follows:[6]

$$\rho c\frac{\partial T}{\partial t} + \nabla \cdot (k\nabla T) = \rho_b C_b \omega_b (T_b - T) + Q_{met} + Q_{ext} \qquad (1)$$

ρ is the tissue mass density, C is the tissue's specific heat and k is the thermal conductivity. P_b and C_b are the blood's density and blood's specific heat respectively. ω_b is the perfusion rate, T_b the arterial blood temperature, Q_{met} and Q_{ext} are the heat sources from metabolism and spatial heating, respectively. The expressions on the left of the above equation 1 indicate the storage of thermal energy and the diffusion of thermal energy, respectively.[7] The terms to the right of the equation 1 refer to blood perfusion, metabolic heat, and external heat, respectively. Numerical Solution of the Pennes equation in cylindrical coordinates can be obtained as follows:

$$\frac{\rho c\,\partial \overline{T}}{\partial t} = k\{\nabla^2 \overline{T}\} - \rho_b C_b \omega_b (\overline{T}) + P(r,\theta) \qquad (2)$$

$$\overline{T}(r,\theta,t) = \Omega(r,\theta,t) + \Lambda(r,\theta) \qquad (3)$$

By placing the equation 2 in 3, the following two equations are obtained:

$$\frac{\rho c\,\partial \Omega(r,\theta,t)}{\partial t} = k\{\nabla^2 \Omega(r,\theta,t)\} - \rho_b C_b \omega_b \Omega(r,\theta,t) \qquad (4)$$

$$k\{\nabla^2 \Lambda(r,\theta)\} - \rho_b C_b \omega_b \Lambda(r,\theta) + P(r,\theta) = 0 \qquad (5)$$

Using the method of separation of variables, we have:

$$\Lambda(r,\theta) = f(r)\sum_{n=0}\cos(n\theta) + g(r)\sum_{n=1}\sin(n\theta) \qquad (6)$$

By placing Equation 6 in Equation 5, the following two equations are obtained:

$$r^2\frac{d^2 f(r)}{dr^2} + r\frac{df(r)}{dr} + (\lambda^2 r^2 - n^2)f(r) = 0 \qquad (7)$$

$$r^2\frac{d^2g(r)}{dr^2}+r\frac{dg(r)}{dr}+(\lambda^2r^2-m^2)g(r)=0 \quad (8)$$

Since the equations 7 and 8 are Bessel differential equations. We have:

$$\Lambda(r,\theta)=(\sum_{n=0}\{A_nJ_{(n,\lambda r)}+C_nN_{(n,\lambda r)}\}\cos(n\theta)+\sum_{m=1}\{B_mJ_{(m,\lambda r)}+C_mN_{(m,\lambda r)}\}\sin(m\theta)) \quad (9)$$

:

$$\Omega(r,\theta,t)=((\sum_{n=0}\{E_nJ_{(n,\lambda r)}+F_nN_{(n,\lambda r)}\}\cos(n\theta)+\sum_{m=1}\{G_mJ_{(m,\lambda r)}+H_mN_{(m,\lambda r)}\}\sin(m\theta)))\{\exp(\frac{\frac{\omega_b\rho_b}{k}-\lambda^2}{\rho c/_k}t)\} \quad (10)$$

So T (r, θ, t) is obtained in this way

$$T(r,\theta,t)=\left((\sum_{n=0}\{E_nJ_{(n,\lambda r)}\}\cos(n\theta)+\sum_{m=1}\{G_mJ_{(m,\lambda r)}\}\sin(m\theta))\right)\left\{\exp\left(\frac{\frac{\omega_b\rho_b}{k}-\lambda^2}{\rho c/_k}t\right)\right\}+(\sum_{n=0}\{A_nJ_{(n,\lambda r)}\}\cos(n\theta)+\sum_{m=1}\{B_mJ_{(m,\lambda r)}\}\sin(m\theta)) \quad (11)$$

2.Hyperthermia treatment calculations without laser

Figure 1 shows the temperature distribution diagrams in terms of position and time at different angles, 45, 60, 72 and 144 for the three nanoparticles Fe_3O_4, $NiFe_2O_4$, and CoFe2O4 in 5 different tissues of brain, bone, muscle, liver and breast. By studding all these graphs, we see that the temperature distribution graph is descending or in other words the temperature distribution in different tissues reduce slowly. [8] It drops suddenly near the surface of the skin due to direct skin contact with the environment. The temperature at any point in the tissue near the center of the cancerous tissue in the upper conduction is less than that in the lower conduction. This means that during heat treatment, there is a high temperature transfer in and around the cancerous tissue. [9] While moving away from the center of the cancerous tissue, the temperature drops. As a consequence, the area near the heat source has the maximum temperature. [10] So, it has the most tissue damage. In general, the maximum temperature serves as a limiting factor in hyperthermia and when it increases, the probability of injury and swelling are high. Therefore, even a small error can exert a significant effect on the amount of tissue damage.

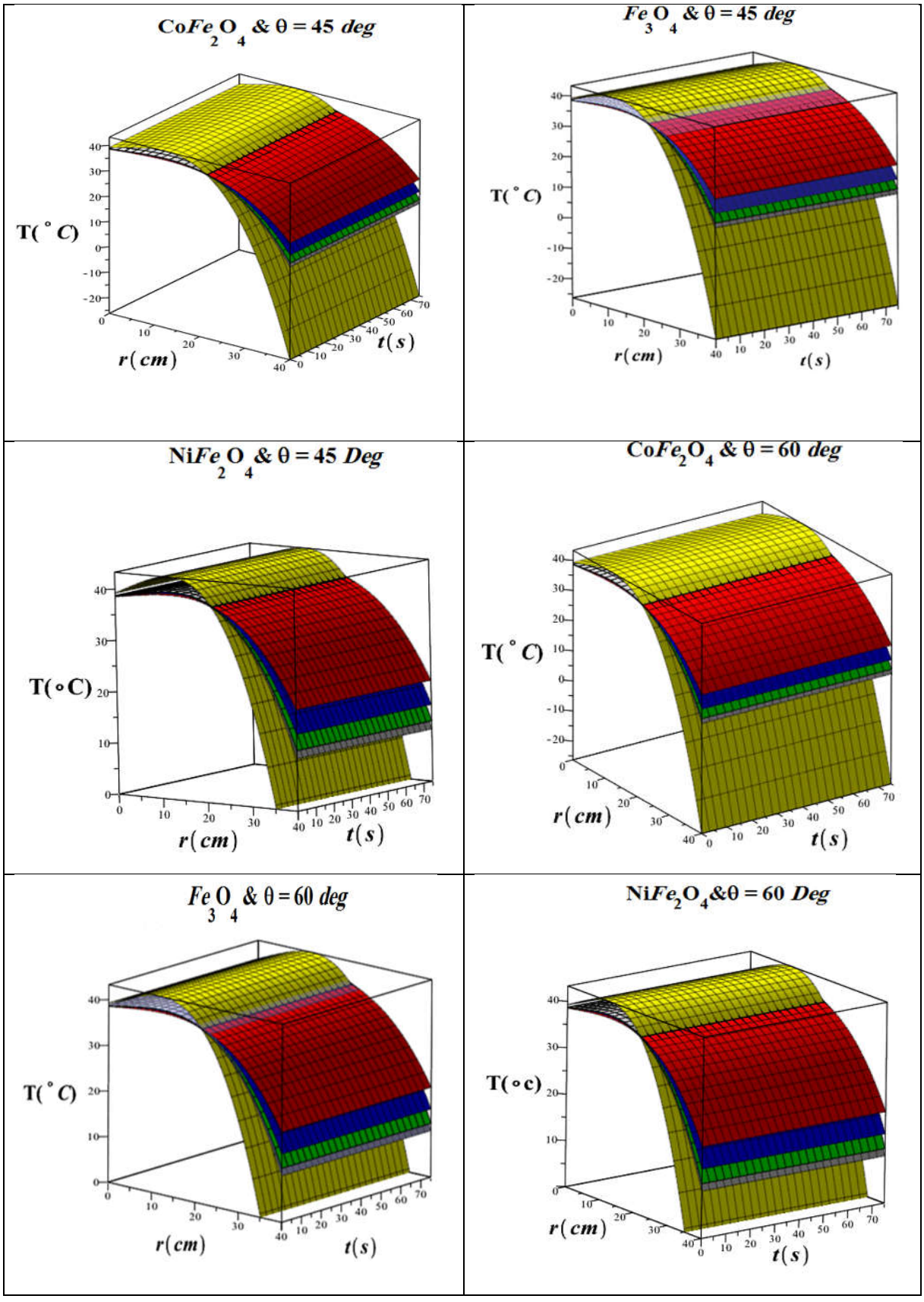
CoFe2O4 & θ = 45 deg
T(°C)
r(cm)
t(s)
Fe3O4 & θ = 45 deg
T(°C)
r(cm)
t(s)
NiFe2O4 & θ = 45 Deg
T(∘C)
r(cm)
t(s)
CoFe2O4 & θ = 60 deg
T(°C)
r(cm)
t(s)
Fe3O4 & θ = 60 deg
T(°C)
r(cm)
t(s)
NiFe2O4&θ = 60 Deg
T(∘c)
r(cm)
t(s)

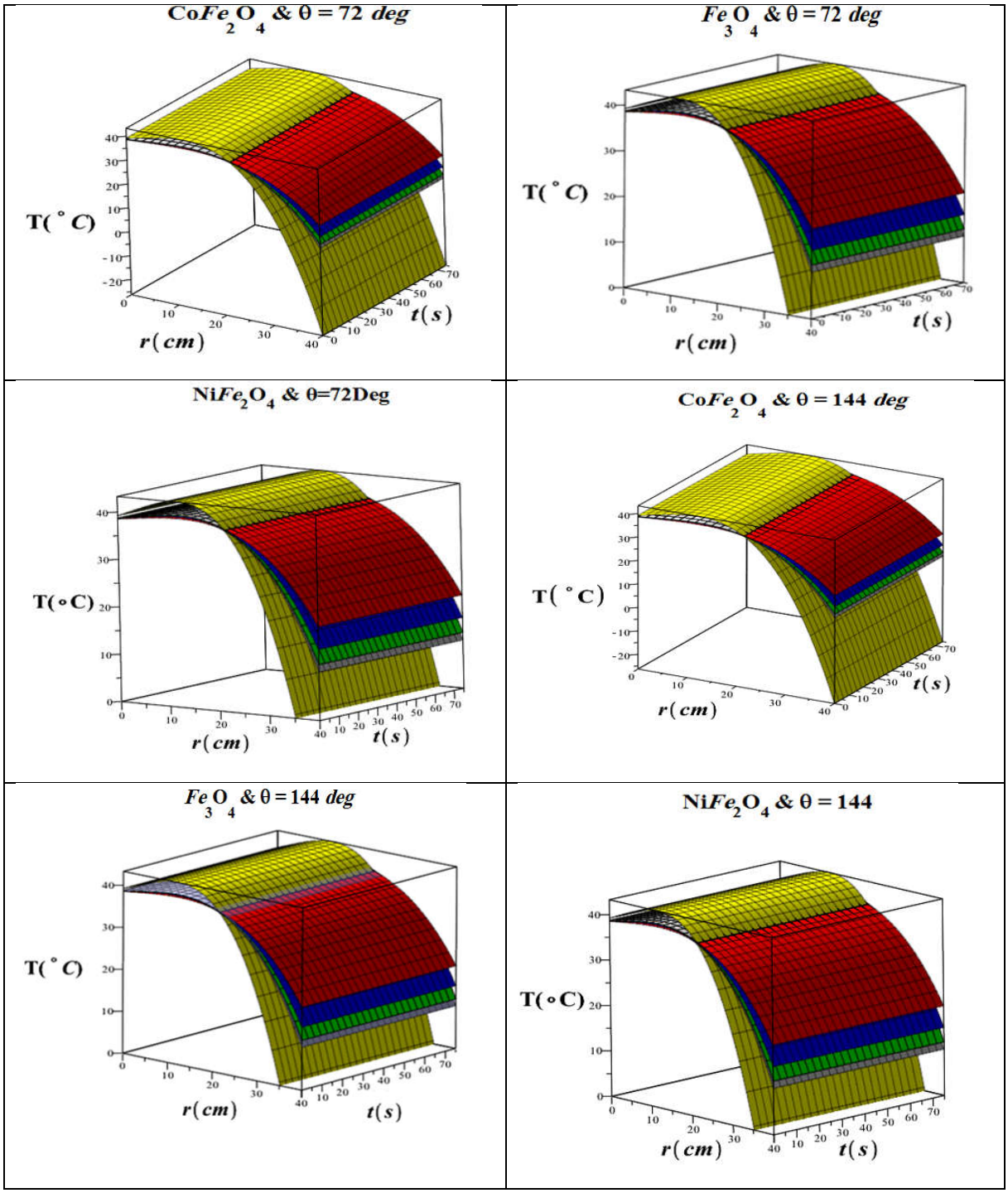
CoFe2O4 & θ = 72 deg
Fe3O4 & θ = 72 deg
NiFe2O4 & θ=72Deg
CoFe2O4 & θ = 144 deg
Fe3O4 & θ = 144 deg
NiFe2O4 & θ = 144
T(°C)
r(cm)
t(s)

Figure 1 - Diagram of temperature distribution According to position and time at angles of 45, 60, 72 and 144 degrees for brain tissue (blue), bone (yellow), muscle (gray), liver (green) and breast (red) In three nanoparticles Fe_3O_4, $CoFe_2O_4$ and $NiFe_2O_4$

Figure 1 demonstrates that the temperature distribution among various tissues is quite similar. Comparing this approach with other methods suggests that utilizing the Pennes equation to estimate temperature distribution within tissue depth is an appropriate method. It is evident that tissue temperature reaches a maximum of 38.5 degrees Celsius, and as mentioned earlier, there are slight variations in temperature among different tissues. Notably, the chart reveals that the breast, brain, and liver experience the highest temperatures, respectively, which aligns with findings from previous research. [7]

Figure 2 demonstrates a three-dimensional diagram of the temperature distribution in terms of position and time for the three nanoparticles $NiFe_2O_4$, $CoFe_2O_4$ and Fe_3O_4 at zero-angle heat therapy. The graphs show that the temperature transfer near cancerous tissue reaches the highest level compared to other tissues. This indicates that there is a higher temperature distribution in cancerous tissue. According to the diagrams, the transfer temperature reaches 38.5 degrees Celsius. [12-18] This suggests that the temperature in cancerous tissue can reach relatively high levels. NiFe2O4 nanoparticles have the highest temperature distribution in cancerous tissue, while CoFe2O4 nanoparticles have the lowest temperature distribution in tissue. [19-24] This implies that NiFe2O4 nanoparticles are more effective in generating heat and raising the temperature in cancerous tissue compared to CoFe2O4. NiFe2O4 nanoparticles show a faster rate of temperature drop compared to other nanoparticles, indicating that they cool down more quickly. On the other hand, CoFe2O4 nanoparticles have a slower rate of temperature drop compared to other nanoparticles. [25-29] Overall, these findings suggest that using NiFe2O4 nanoparticles could potentially be more effective for heating up cancerous tissues and achieving higher temperatures, while CoFe2O4 nanoparticles may not generate as much heat or reach high temperatures as quickly.

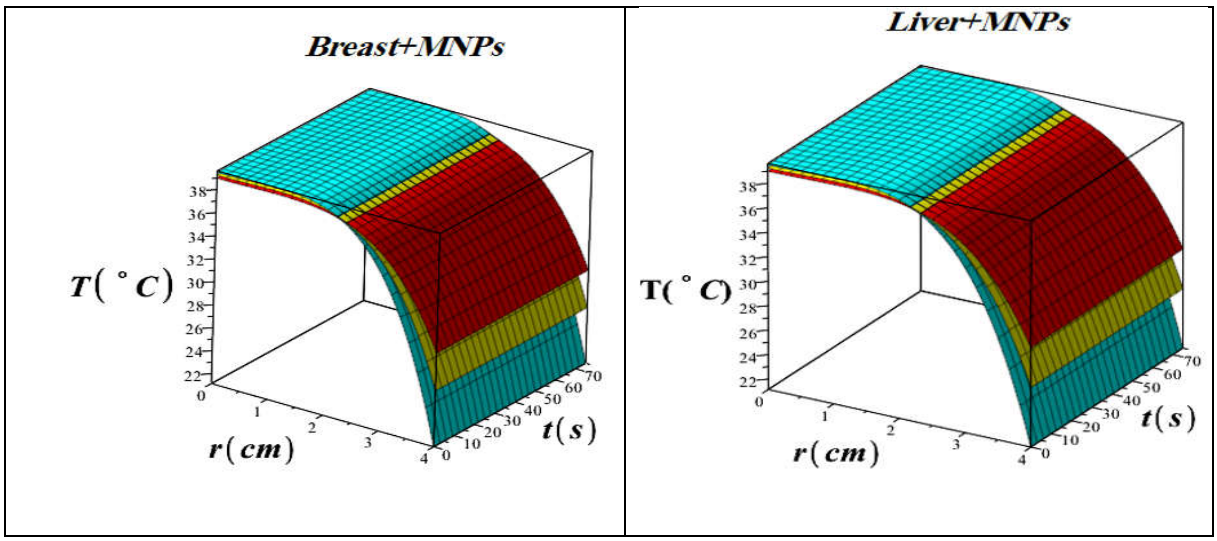

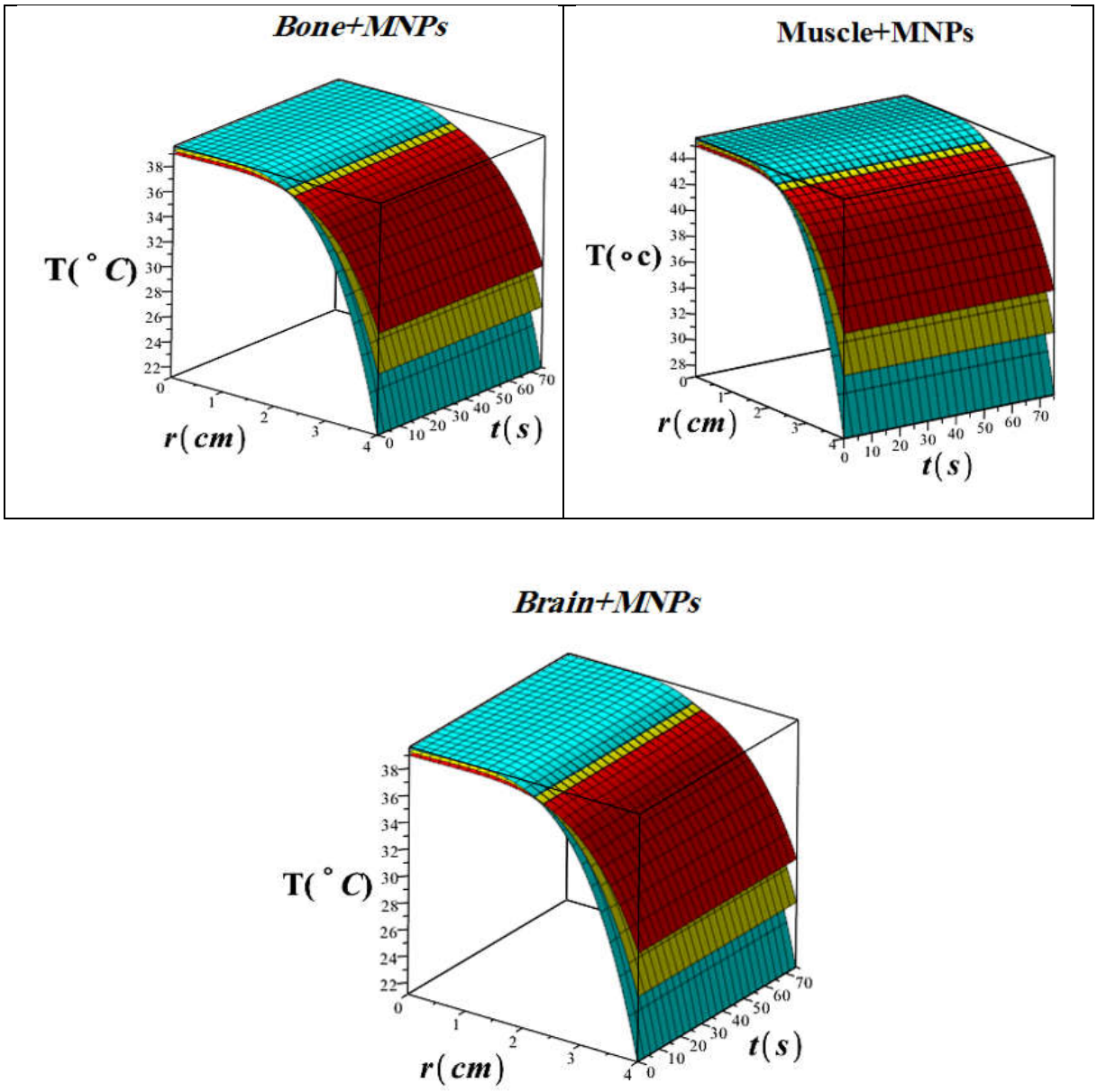

Figure 2- Three-dimensional diagram of temperature distribution in terms of place and time at zero-degree angle with injection of three magnetic nanoparticles $NiFe_2O_4$ (blue), $CoFe_2O_4$ (red) and Fe_3O_4 (yellow) in heat therapy for liver and breast, Muscle, bone and brain cancer tissues

Figure 3 illustrates that, while the temperature changes in the cancerous tissue change with variation of angle and position. Hence this graph fluctuates. Evaluations, demonstrates that the highest temperatures are intended to the angles of 0, 50, 100, 150 200 and 250 degrees. In other term, at these angles, there is the highest temperature distribution in the tissue. Also, the lowest values of temperature distribution are at angles 11, 68, 118, 174 and 225. What is more, $NiFe_2O_4$ nanoparticles have the highest temperature distribution whereas $CoFe_2O_4$ has the lowest temperature distribution.

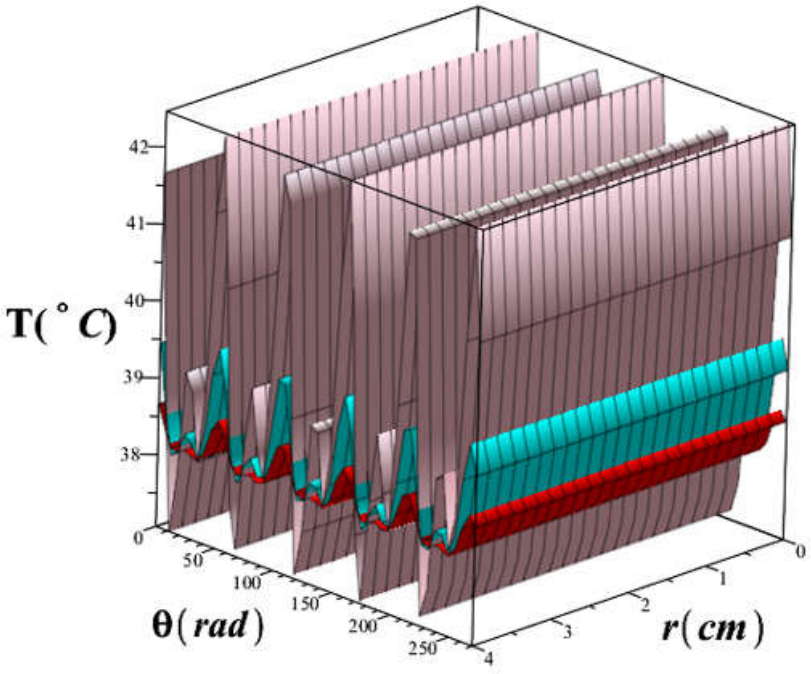

Figure 3 - 3D diagram of temperature distribution in terms of angle and position for three nanoparticles of $NiFe_2O_4$, $CoFe_2O_4$ and Fe_3O_4 in brain tissue in 750 seconds. The colors of Purple, blue and red indicate $NiFe_2O_4$, Fe_3O_4 and $CoFe_2O_4$, respectively.

3.Calculations for the use of laser and magnetic nanoparticles in hyperthermia simultaneously

In this section, we consider the use of lasers and nanoparticles in order to destroy cancer cells in hyperthermia. Figure 5 shows three-dimensional diagrams of the temperature distribution in terms of position and time using three nanoparticles $NiFe_2O_4$, $CoFe_2O_4$ and Fe_3O_4 and laser in bone, brain, breast, liver and muscle tissues. The graphs illustrate that application of lasers can increases the temperature by several degree hyperthermia ,in general. Specifically, with the use of lasers, the temperature of the tissue has experienced a growth about 4.5 degrees compared to the case without lasers. As a consequence, when both magnetic nanoparticles and laser are used in hyperthermia, cancer cells which are more sensitive to healthy tissue are quickly destroyed.

.

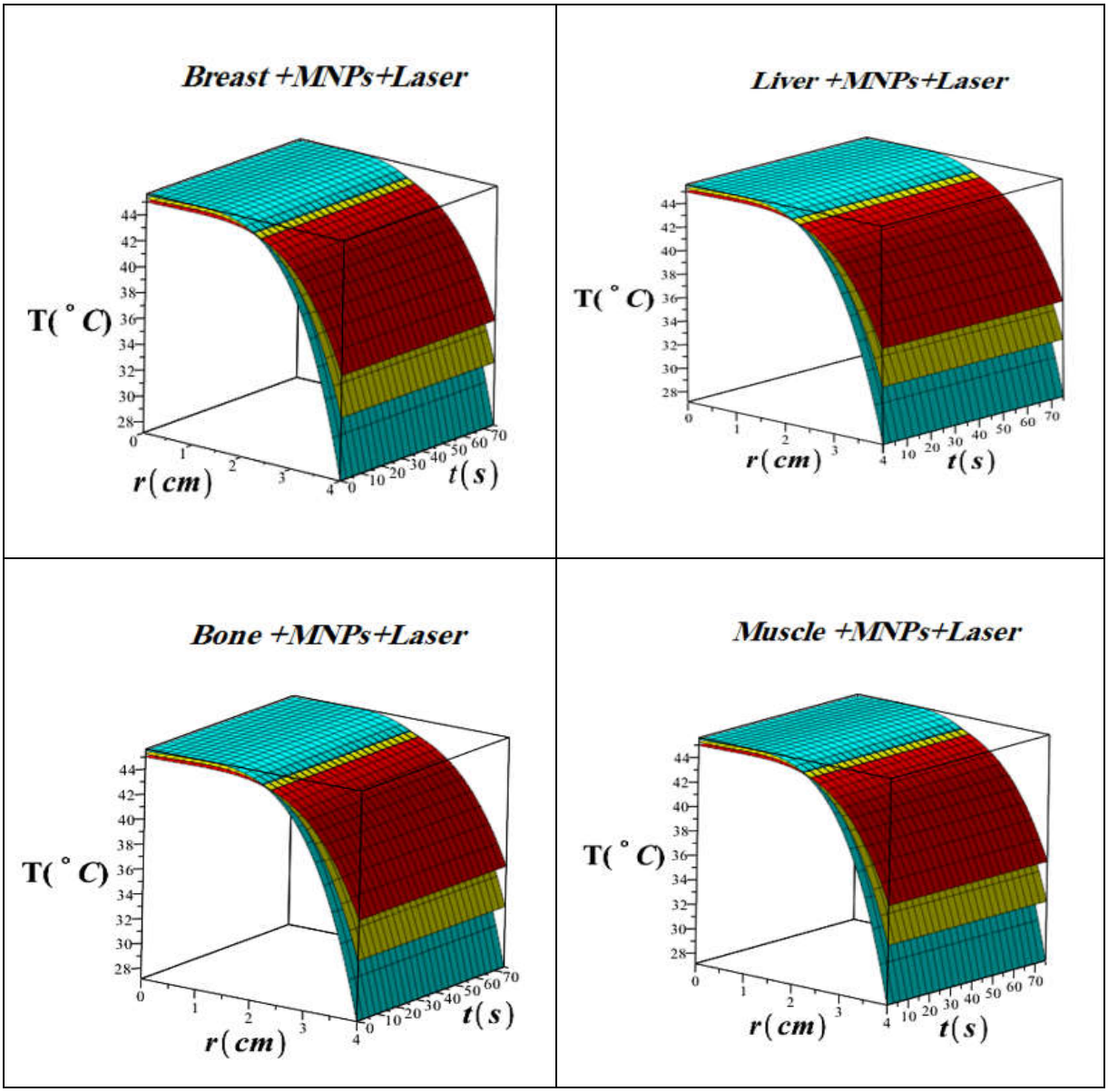
Breast +MNPs+Laser
T(° C)
r(cm)
t(s)
Liver +MNPs+Laser
T(° C)
r(cm)
t(s)
Bone +MNPs+Laser
T(° C)
r(cm)
t(s)
Muscle +MNPs+Laser
T(° C)
r(cm)
t(s)

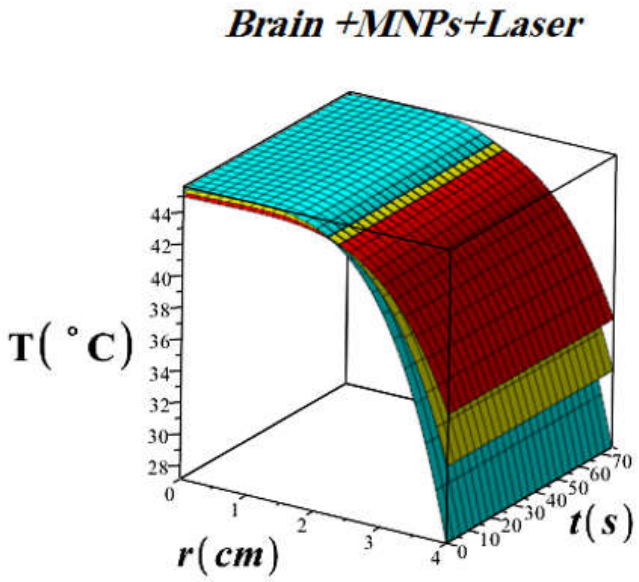

Figure 4 - 3D diagrams of temperature distribution according to position and time using laser and three nanoparticles $NiFe_2O_4$ (blue), $CoFe_2O_4$ (red) and Fe_3O_4 (yellow) in bone, brain, liver, breast and Muscle.

Figure 5 shows a three-dimensional diagram of the temperature distribution in terms of angle and time variations. This diagram is drawn by considering the laser with nanoparticles in the brain tissue. Although the graph process is the same as the laser-free graph, the use of lasers has raised the temperature by about 4.5 degrees.

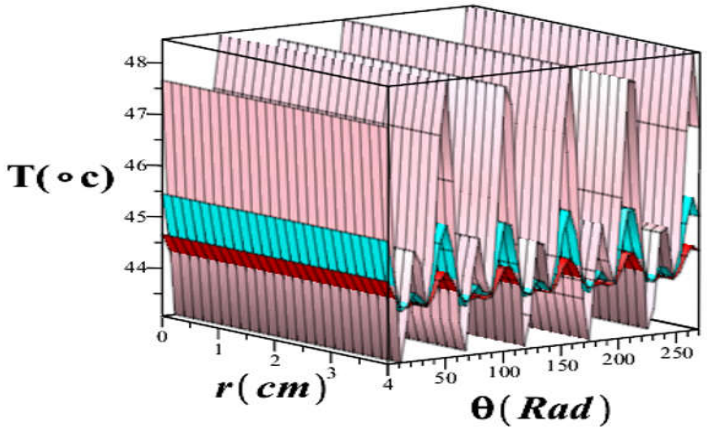

Figure 5- Three-dimensional diagram of temperature distribution in terms of angle and position for three nanoparticles $NiFe_2O_4$, $CoFe_2O_4$ and Fe_3O_4 In the brain tissue in 750 seconds and the simultaneous use of laser. Purple, blue and red colors originate $NiFe_2O_4$, Fe_3O_4 and $CoFe_2O_4$, respectively.

4.Conclusions

In this article, for the first time, we have studied how heat is distributed in different Cancerous organs of the brain, liver, bone, human muscle, etc. using three different magnetic nanoparticles. Heat exchange processes and their equations are completely described in this paper. By examining these equations and related diagrams, it can be concluded that the use of the pennes equation in estimating the temperature distribution in the depth of tissue is a suitable method. We also see that the temperature of the tissues reaches a maximum of 38.5 ° C and the temperature has experienced slightly difference for different tissues which is in agreement with the results obtained in previous research. We also found that $NiFe_2O_4$ nanoparticles have the highest temperature distribution in cancerous tissue compared to other nanoparticles. Another conclusion was that temperature changes in cancerous tissue change with variations of angle. Specifically, it is not always possible to expect that either maximum temperature or uniform temperature to reach the desired cancer cell. The highest values of temperature at angles of 0, 50, 100, 150, 200 and 250 degrees are transferred to cancer cells. Because Of the fact that the slightest mistake in determining the injection distance of the magnetite nanoparticle destroys the healthy tissue around the tumor, It is absolutely important how far the magnetic nanoparticles are injected from the tumor. It can be boldly said that the distribution of nanoparticles is one of the most significant factors affecting the final temperature distribution of tissue. Also, increasing time or energy consumption (heat delivery to the tissue) may result in irreversible damages to healthy tissue. Also considering the Pennes equation, it can be said that blood flow also serves a decisive role in the distribution of temperature in the tissue. Of course, the equation of the pennes cannot explain the phenomenon of heat exchange between blood vessels. Therefore, it is necessary to modify this model slightly to overcome these weaknesses. What is more, to increase the temperature in hyperthermia, a laser can be used at the same time in order to enhance the temperature of the tissue and the demolition of cancer cells is done quickly. According to our calculations, by simultaneous use of laser and magnetic nanoparticles, the temperature of cancerous tissue rises up to 44 or 45 degrees. In addition, the use of alternating magnetic fields deters from the destruction of healthy tissues. So, generally, the best possible treatment for eradication of cancer cells is obtained when the appropriate magnetic nanoparticles, external magnetic field and laser are used simultaneously. More studies need to be done to find the optimal substance that can produce the most heat to improve treatment results. Whereas, a number of clinical and preclinical trials have been performed to test the feasibility of this new treatment, there are still many unanswered issues in order to transfer of this technology from theory to practice .Because of fact that working in this field requires expertise in several fields, progress in hyperthermia specialists in various fields, including physicians, biologists, chemists, physicists, engineers, and so on should participate together. In the first stage to make progress in this area, Planning, implementation, monitoring and optimization of treatment should be considered.

References

(1) Wang, Wei, et al. "Surface diffusion-limited lifetime of silver and copper nanofilaments in resistive switching devices." Nature communications 10.1 (2019): 81.

(2) Dahl, Olav, and Jens Overgaard. "A century with hyperthermic oncology in Scandinavia." Acta Oncologica 34.8 (1995): 1075-1083.
(3) Pennes, Harry H. "Analysis of tissue and arterial blood temperatures in the resting human forearm." Journal of applied physiology 85.1 (1998): 5-34
(4) Park, Gimin, et al. "Modeling heat transfer in humans for body heat harvesting and personal thermal management." Applied Energy 323 (2022): 119609.

(5) Yue, Kai, Xinxin Zhang, and Fan Yu. "An analytic solution of one-dimensional steady-state Pennes' bioheat transfer equation in cylindrical coordinates." Journal of thermal Science 13 (2004): 255-258.

(6) Wissler, E. H. "Comments on Weinbaum and Jiji's discussion of their proposed bioheat equation." (1987): 355-356.

(7) Gas, Piotr. "Tissue temperature distributions for different frequencies derived from interstitial microwave hyperthermia." Przegląd Elektrotechniczny 88.12b (2012): 131-134.

(8) Naseri, N.; Valizadeh, H.; Zakeri-Milani, P. Solid Lipid Nanoparticles and Nanostructured Lipid Carriers: Structure Prepara-tion and Application. Adv. Pharm. Bull. 2015, 5, 305.

(9) Pooja, D.; Tunki, L.; Kulhari, H.; Reddy, B. B.; Sistla, R.Optimization of Solid Lipid Nanoparticles Prepared by a Single Emulsification-Solvent Evaporation Method. Data Brief 2016, 6, 15.

(10) Tian, Q.-h.; Ning, W.-b.; Wang, W.-j.; Yuan, X.-h.; Bai, Z.-m.Synthesis of Size-Controllable Fe3O4 Magnetic Submicroparticles and Its Biocompatible Evaluation in Vitro. J. Cent. South Univ. 2016,23, 2784.

(11) Mahmoudi, M.; Sant, S.; Wang, B.; Laurent, S.; Sen, T.Superparamagnetic Iron Oxide Nanoparticles (SPIONs): Develop-ment, Surface Modification and Applications in Chemotherapy. Adv.Drug Delivery Rev. 2011, 63, 24.

(12) Lee, N.; Hyeon, T. Designed Synthesis of Uniformly Sized Iron Oxide Nanoparticles for Efficient Magnetic Resonance Imaging Contrast Agents. Chem. Soc. Rev. 2012, 41, 2575.

(13) Gallo, J.; Long, N. J.; Aboagye, E. O. Magnetic Nanoparticles as Contrast Agents in the Diagnosis and Treatment of Cancer. Chem.Soc. Rev. 2013, 42, 7816.

(14) Josephson, L.; Lewis, J.; Jacobs, P.; Hahn, P. F.; Stark, D. D.The Effects of Iron Oxides on Proton Relaxivity. Magn. Reson. Imaging 1988, 6,647

15) Laurent, S.; Dutz, S.; Häfeli, U. O.; Mahmoudi, M. Magnetic Fluid Hyperthermia: Focus on Superparamagnetic Iron Oxide Nanoparticles. Adv. Colloid Interface Sci. 2011, 166, 8.

(16) Sadat, M. E.; Patel, R.; Sookoor, J.; Bud'Ko, S. L.; Ewing, R. C.;Zhang, J.; Xu, H.; Wang, Y.; Pauletti, G. M.; Mast, D. B.; Shi, D. Effect of Spatial Confinement on Magnetic Hyperthermia via Dipolar Interactions in Fe3O4 Nanoparticles for Biomedical Applications.Mater. Sci. Eng., C 2014, 42, 52.

(17) Sadat, M. E.; Patel, R.; Bud'Ko, S. L.; Ewing, R. C.; Zhang, J.;Xu, H.; Mast, D. B.; Shi, D. Dipole-Interaction Mediated Hyper-thermia Heating Mechanism of Nanostructured Fe3O4 Composites.Mater. Lett. 2014, 129, 57.

(18) Zhou, Z.; Yang, L.; Gao, J.; Chen, X. Structure−Relaxivity Relationships of Magnetic Nanoparticles for Magnetic Resonance Imaging. Adv. Mater. 2019, No. 1804567.

(19) Coral, D. F.; Mendoza Zélis, P.; Marciello, M.; Morales, M. D. P.; Craievich, A.; Sánchez, F. H.; Fernández Van Raap, M. B. Effect of Nanoclustering and Dipolar Interactions in Heat Generation for Magnetic Hyperthermia. Langmuir 2016, 32, 1201.

(20) Geng, S.; Yang, H.; Ren, X.; Liu, Y.; He, S.; Zhou, J.; Su, N.; Li,Y.; Xu, C.; Zhang, X.; Cheng, Z. Anisotropic Magnetite Nanorods for Enhanced Magnetic Hyperthermia. Chem. Asian J. 2016, 11, 2996.

(21) Mohapatra, J.; Zeng, F.; Elkins, K.; Xing, M.; Ghimire, M.;Yoon, S.; Mishra, S. R.; Liu, J. P. Size-Dependent Magnetic and Inductive Heating Properties of Fe3O4 Nanoparticles: Scaling Laws across the Superparamagnetic Size. Phys. Chem. Chem. Phys. 2018, 20,12879.

(22) Carroll, M. R. J.; Huffstetler, P. P.; Miles, W. C.; Goff, J. D.;Davis, R. M.; Riffle, J. S.; House, M. J.; Woodward, R. C.; St Pierre, T.G. The Effect of Polymer Coatings on Proton Transverse Relaxivities of Aqueous Suspensions of Magnetic Nanoparticles. Nanotechnology 2011, 22, No. 325702.

(23) German, S. V.; Navolokin, N. A.; Kuznetsova, N. R.; Zuev, V.V.; Inozemtseva, O. A.; Anis'kov, A. A.; Volkova, E. K.; Bucharskaya,A. B.; Maslyakova, G. N.; Fakhrullin, R. F.; Terentyuk, G. S.;Vodovozova, E. L.; Gorin, D. A. Liposomes Loaded with Hydrophilic Magnetite Nanoparticles: Preparation and Application as Contrast Agents for Magnetic Resonance Imaging. Colloids Surf., B 2015, 135,109.

(24) Abbasi, A. Z.; Gutiérrez, L.; Del Mercato, L. L.; Herranz, F.;Chubykalo-Fesenko, O.; Veintemillas-Verdaguer, S.; Parak, W. J.;Morales, M. P.; González, J. M.; Hernando, A.; De La Presa, P.Magnetic Capsules for NMR Imaging: Effect of Magnetic Nano-particles Spatial Distribution and Aggregation. J. Phys. Chem. C 2011,115, 6257.

(25) Jiménez-López, J.; García-Hevia, L.; Melguizo, C.; Prados, J.;Bañobre-López, M.; Gallo, J. Evaluation of Novel Doxorubicin-Loaded Magnetic Wax Nanocomposite Vehicles as Cancer Combinatorial Therapy Agents. Pharmaceutics 2020, 12, No. 637.

(26) Calucci, L.; Grillone, A.; Riva, E. R.; Mattoli, V.; Ciofani, G.;Forte, C. NMR Relaxometric Properties of SPION-Loaded Solid Lipid Nanoparticles. J. Phys. Chem. C 2017, 121, 823.

(27) Lu, C. Y.; Ji, J. S.; Zhu, X. L.; Tang, P. F.; Zhang, Q.; Zhang, N.N.; Wang, Z. H.; Wang, X. J.; Chen, W. Q.; Hu, J. B.; Du, Y. Z.; Yu, R.S. T2-Weighted Magnetic Resonance Imaging of Hepatic Tumor Guided by SPIO-Loaded Nanostructured Lipid Carriers and Ferritin Reporter Genes. ACS Appl. Mater. Interfaces 2017, 9, 35548.

(28) Chen, B.; Xing, J.; Li, M.; Liu, Y.; Ji, M. DOX@Ferumoxytol-Medical Chitosan as Magnetic Hydrogel Therapeutic System for Effective Magnetic Hyperthermia and Chemotherapy in Vitro.Colloids Surf., B 2020, 190, No. 110896.

(29) Carvalho, A.; Gallo, J.; Pereira, D. M.; Valentão, P.; Andrade, P.B.; Hilliou, L.; Ferreira, P. M. T.; Bañ obre-López, M.; Martins, J. A.Magnetic Dehydrodipeptide-Based Self-Assembled Hydrogels for Theragnostic Applications. Nanomaterials 2019, 9, No. 541.